RESEARCH ARTICLE
PLANETARY SCIENCES

Earth and Planetary Physics
4: 11–16, 2020
doi: 10.26464/epp2020009

A MAVEN investigation of O^{++} in the dayside Martian ionosphere

Hao Gu[1], Jun Cui[2,3,4*], ZhaoGuo He[2,3], and JiaHao Zhong[2]

[1]State Key Laboratory of Lunar and Planetary Sciences, Macau University of Science and Technology, Macau 999078, China;

[2]School of Atmospheric Sciences, Sun Yat-sen University, Zhuhai Guangdong 519082, China;

[3]Chinese Academy of Sciences Center for Excellence in Comparative Planetology, Hefei 230000, China;

[4]National Astronomical Observatories, Chinese Academy of Sciences, Beijing 100012, China

Key Points:

- Primary sources and sinks of O^{++} show interesting variations with altitudes
- An exact balance between O^{++} production and destruction is suggested by the data below 200 km
- The discrepancy from local photochemical equilibrium at higher altitudes implies the existence of strong O^{++} escape

Citation: Gu, H., Cui, J., He, Z. G., and Zhong, J. H. (2020). A MAVEN investigation of O^{++} in the dayside Martian ionosphere. *Earth Planet. Phys.*, *4*(1), 11–16. http://doi.org/10.26464/epp2020009

Abstract: O^{++} is an interesting species in the ionospheres of both the Earth and Venus. Recent measurements made by the Neutral Gas and Ion Mass Spectrometer (NGIMS) on board the Mars Atmosphere and Volatile Evolution (MAVEN) spacecraft provide the first firm detection of O^{++} in the Martian ionosphere. This study is devoted to an evaluation of the dominant O^{++} production and destruction channels in the dayside Martian ionosphere, by virtue of NGIMS data accumulated over a large number of MAVEN orbits. Our analysis reveals the dominant production channels to be double photoionization of O at low altitudes and photoionization of O^+ at high altitudes, respectively, in response to the varying degree of O ionization. O^{++} destruction is shown to occur mainly via charge exchange with CO_2 at low altitudes and with O at high altitudes. In the dayside median sense, an exact balance between O^{++} production and destruction is suggested by the data below 200 km. The apparent discrepancy from local photochemical equilibrium at higher altitudes is interpreted as a signature of strong O^{++} escape on Mars, characterized by an escape rate of 6×10^{22} s^{-1}.

Keywords: Mars; ionosphere; doubly ionized oxygen; MAVEN

1. Introduction

Since firm detection of O^{++} in the ionospheres of the Earth (Breig et al., 1977) and Venus (Taylor et al., 1980), considerable research efforts have been devoted to the identification of the dominant chemical sources and sinks of this interesting ion species. Assuming that the destruction of O^{++} proceeds exclusively via charge exchange with O, Breig et al. (1977) identified the main sources of O^{++} in the terrestrial ionosphere as photoionization of O^+ and Auger stabilized K shell ionization of O by X ray photons. Motivated by laboratory measurements of large reaction rates for the destruction of O^{++} by N_2 and O_2 (Johnsen and Biondi, 1978; Howorka et al., 1979), Victor and Constantinides (1979) argued that double photoionization of O outer shell electrons was much more efficient in producing ionospheric O^{++}. As the only multiply charged constituent that has, so far, been detected at Venus and Earth (Ghosh et al., 1995, Thissen et al., 2011), O^{++} is particularly attractive to aeronomers because of the large energy required for its formation. It also serves as a useful diagnostic of solar irradiance at short wavelengths, especially the enhancement in solar flux during solar disturbances. In addition, the double charge of this ion species causes thermal diffusion to be an especially effective mode of transport for O^{++} at high altitudes (Geiss et al., 1978, Geiss and Young, 1981, Breig et al., 1982). In the Venusian ionosphere, O^{++} is produced via the same process and lost via charge exchange reactions with CO_2, CO, N_2 and O (Fox and Victor, 1981). These reactions also serve as important production channels of N^+ and C^+ in the Venusian ionosphere, especially above 200 km (Fox and Victor, 1981).

Nonetheless, systemic observations and studies of O^{++} on Mars, with similar atmospheric components as on Venus, have not yet been performed. Recently, extensive measurements made by the Neutral Gas and Ion Mass Spectrometer (NGIMS) (Mahaffy et al., 2015a) on board the Mars Atmosphere and Volatile Evolution (MAVEN) spacecraft provided the first detection of O^{++} in the Martian ionosphere (Jakosky et al., 2015). For a solar zenith angle (SZA) of 60°, O^{++} distribution peaks at 300 km with a density of around 0.5 cm^{-3} and declines to 0.1 cm^{-3} at 500 km (Benna et al., 2015). These new data allow us to validate the O^{++} photochemistry proposed to interpret the ionospheric O^{++} observations on both the Earth and Venus, motivating the present study.

2. O^{++} Photochemistry

The various O^{++} production mechanisms considered in this study

Correspondence to: J. Cui, cuijun7@mail.sysu.edu.cn
Received 28 SEP 2019; Accepted 15 NOV 2019.
Accepted article online 04 DEC 2019.

include photoionization of O^+ (Breig et al., 1977) and double photoionization of O (Victor and Constantinides, 1979), of which the latter also inherently includes Auger stabilized K shell ionization of O. We further assume that O^{++} destruction proceeds mainly via charge exchange reactions with four abundant species of the Martian upper atmosphere, CO_2, O, CO, and N_2 (Mahaffy et al., 2015b).

The photoionization rate of O^+, $P^{\rm pi}_{O^+}$ is obtained from

$$P^{\rm pi}_{O^+}(z) = n_{O^+}(z)\int_0^{\lambda_{O^+}} F_\infty(\lambda)e^{-\tau(z,\lambda)}\sigma^{\rm pi}_{O^+}(\lambda){\rm d}\lambda, \quad (1)$$

where z is the altitude, n_{O^+} is the O^+ number density, λ is the wavelength, F_∞ is the threshold wavelength for photoionization of O^+, F_∞ is the solar radiation flux at the top of the atmosphere, $\sigma^{\rm pi}_{O^+}$ is the photoionization cross section of O^+, τ is the optical depth given by

$$\tau(z,\lambda) = \sum\nolimits_i \sigma^a_i(\lambda)\int_0^\infty n_i(z)\sec\theta{\rm d}z, \quad (2)$$

with θ being the SZA, n_i being the number density of the ith neutral species, and σ^a_i is the respective photoabsorption cross section. Similarly, the double photoionization rate of O, $P^{\rm pi}_{O'}$ is formulated as

$$P^{\rm pi}_{O}(z) = n_{O}(z)\int_0^{\lambda_{O}} F_\infty(\lambda)e^{-\tau(z,\lambda)}\sigma^{\rm pi}_{O}(\lambda){\rm d}\lambda, \quad (3)$$

where $\sigma^{\rm pi}_{O}$ is the double photoionization cross section of O, and λ_O is the threshold wavelength for double photoionization of O. In this study, the photoabsorption and double photoionization cross sections are adapted from the previous compilation by some of us (Cui J et al., 2011); the photoionization cross section of O^+ is taken from Henry (1968) and Breig et al. (1977).

The destruction rate of O^{++} in the Martian ionosphere via charge exchange with the ith neutral species, denoted as L^{ce}_i, can be calculated by

$$L^{\rm ce}_i(z) = k_i n_{O^{++}}(z)n_i(z), \quad (4)$$

where $n_{O^{++}}$ is the O^{++} number density and k_i is the respective rate coefficient. The rate coefficients required for this study are detailed in Table 1.

Table 1. Chemical destruction channels of O^{++} and the respective rate coefficients

Reaction	Rate coefficient ($cm^3{\cdot}s^{-1}$)	Reference
$O^{++} + CO_2 \rightarrow$ products	2.0×10^{-9}	Fox and Victor (1981)
$O^{++} + O \rightarrow O^+ + O^+$	1.5×10^{-10}	Fox and Victor (1981)
$O^{++} + N_2 \rightarrow$ products	1.6×10^{-9}	Howorka et al. (1979)
$O^{++} + CO \rightarrow$ products	1.6×10^{-9}	Fox and Victor (1981)

3. O^{++} Production and Destruction Rates

Following the photochemical scheme outlined in Section 2, we calculate the O^{++} production and destruction rates in the dayside Martian ionosphere based on the data accumulated over 2,356 MAVEN orbits from September 2014 to December 2017, all with periapsis SZA below 85°. In applying Equations (1)–(4), the incident solar Extreme Ultraviolet (EUV) and X-ray flux is obtained from the solar spectral model at Mars constructed from the Flare Irradiance Spectral Model — Mars and calibrated with the MAVEN Ultraviolet Monitor band irradiance data (Eparvier et al., 2015; Thiemann et al., 2017), whereas the neutral and ion densities are based on the NGIMS measurements in the closed source neutral and open source ion modes, respectively (Mahaffy et al., 2015a). Only the inbound portion of each MAVEN orbit is included in the subsequent analysis to reduce the well-known effect of wall contamination on the NGIMS antechamber walls (e.g., Stone et al., 2018).

Taking MAVEN orbit #5636 on 26 Aug 2017 during the nominal mission phase as an example, we show the characteristics of the dayside Martian upper atmosphere and ionosphere in Figure 1a in terms of the density profiles of four neutral species, CO_2, O, N_2, and CO, as well as two ion species, O^+ and O^{++}, over the altitude range of 150–300 km. The O^+ and O^{++} densities are multiplied by 10^6 and 10^8 to improve visibility. The displayed neutral density profiles are extrapolated to higher altitudes based on the 3rd order polynomial fittings to logarithmic NGIMS densities, as indicated by the solid lines in the figure. The derived O^{++} production and destruction rates are presented in Figure 1c for various channels, with the aid of the solar EUV/X-ray spectrum on top of the atmosphere provided in Figure 1b over the wavelength range of 0.5–190 nm. The vertical dashed and dash-dotted lines indicate the threshold wavelengths for photoionization of O^+ (Henry, 1968) and double photoionization of O (Laher and Gilmore, 1990). During this orbit, the northern mid latitude regions of Mars at SZA ~ 82° were sampled, characterized by draped magnetic field lines away from any strong crustal magnetic anomaly (e.g., Connerney et al., 1999). The corresponding 10.7 cm solar radio index at Earth is 79.2 in solar flux units (10^{-22} W·m^{-2}), reflecting low solar activity conditions.

Figure 1 reveals that O^{++} production is dominated by photoionization of O^+ at high altitudes and by double photoionization of O at low altitudes, respectively. The peak O^{++} production appears deep in the Martian upper atmosphere not sampled during the MAVEN nominal mission phase. Equations 1 and 3 essentially imply that the relative importance of the two production channels depends on the ionized fraction of O in the optically thin regions of the upper atmosphere. According to Figure 1a, such a fraction increases sharply with increasing altitude from 5×10^{-7} at the periapsis altitude of 152 km to 4×10^{-3} at 300 km. It is interesting to note that in the Venusian ionosphere, double photoionization of O is more important than photoionization of O^+ at all altitudes up to at least 260 km (Fox and Victor, 1981), where the ionized fraction of O is also 4×10^{-3} (Taylor et al., 1980; Hedin, 1983). The reason for such an apparent discrepancy is unclear but we speculate it to be, at least in part, linked to the different cross section data used for double photoionization of O between the two studies. Figure 1c further suggests the dominant O^{++} destruction channels to be its charge exchange reaction with CO_2 at low altitudes and with O at high altitudes, respectively. Similar charge exchange reactions with N_2 and CO are everywhere less important but still make non-negligible contributions to O^{++} destruction in the dayside Martian

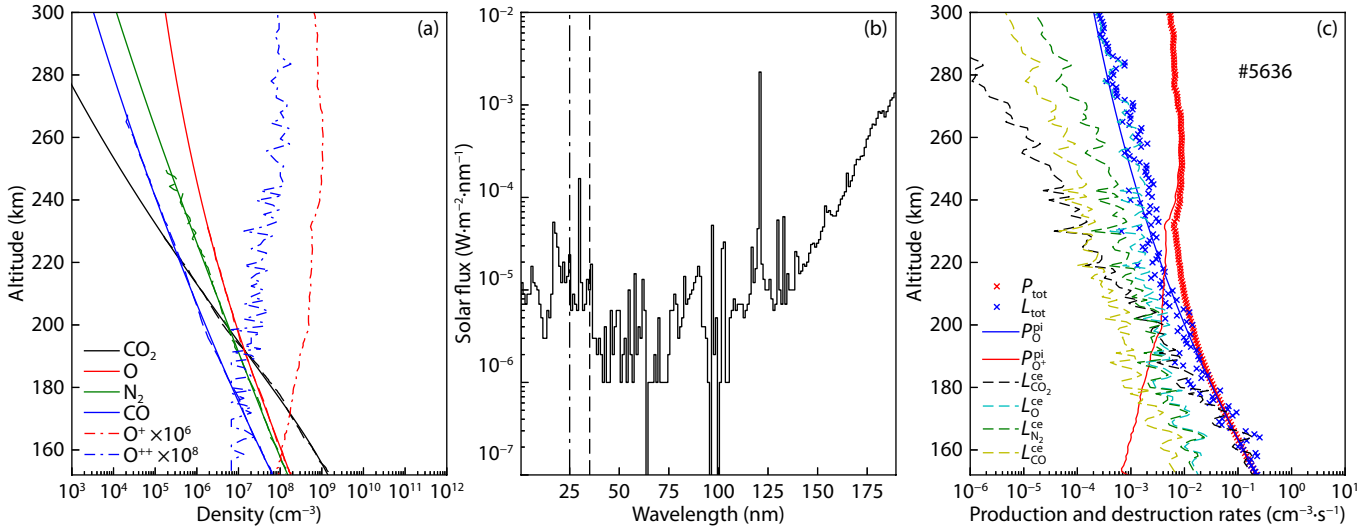

Figure 1. (a) The characteristics of the dayside Martian upper atmosphere and ionosphere for the inbound portion of MAVEN orbit #5636 during the nominal mission phase, in terms of the density profiles of CO_2, O, N_2, CO, O^+, and O^{++}. The 3rd order polynomial best-fits to logarithmic NGIMS neutral densities are also indicated by the solid lines. (b) The solar EUV/X-ray spectrum over the wavelength range of 0.5–190 nm, with the vertical dashed and dash-dotted lines giving the threshold wavelengths for photoionization of O^+ (Henry, 1968) and double photoionization of O (Laher and Gilmore, 1990), respectively. (c) The calculated O^{++} production (solid lines) and destruction (dashed lines) rate profiles for various channels, along with the total production (red cross) and destruction (blue cross) rate profiles.

ionosphere. Of special interest is the near equality between O^{++} production and destruction below 200 km, implying that the condition of local photochemical equilibrium (PCE) should be satisfied.

We compare further in Figure 2 the O^{++} production and destruction rates for various channels at 150–300 km in the dayside median sense, along with the total production and destruction rates. The figure reveals similar trends as demonstrated in Figure 1c for MAVEN orbit #5636. Specifically, double photoionization of O is the dominant O^{++} production channel below 220 km whereas photoionization of O^+ is more important at higher altitudes. For instance, the fractional contribution from O^{++} production via the former process accounts for more than 98% of total production at 160 km, but drops rapidly to about 5% at 300 km. For O^{++} destruction, its charge exchange reactions with CO_2 and O, the two most abundant species of the Martian upper atmosphere (Mahaffy et al., 2015b), serve as the dominant channels below and above 210 km, respectively. To be more specific, O^{++} destruction via charge

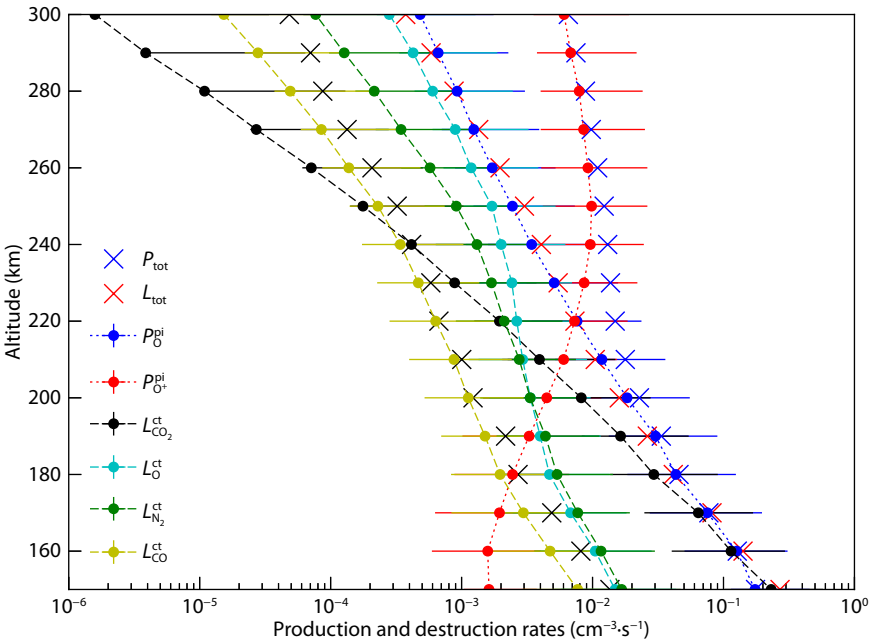

Figure 2. Similar to Figure 1c but for the dayside median situation in the Martian upper atmosphere and ionosphere combining the data from all available MAVEN orbits. For comparison, we also show (with black crosses) the nightside total O^{++} destruction rate (see Section 4 for details).

exchange with CO_2 accounts for about 80% of total destruction at 160 km, while charge exchange with O is responsible for more than 75% of O^{++} destruction at 300 km. A comparison between the total O^{++} production and destruction rates suggests the PCE condition to be satisfied up to at least 200 km, which is also a validation of the O^{++} photochemical scheme proposed in previous studies to interpret the measured concentrations of this species in the ionospheres of both the Earth (Victor and Constantinides, 1979) and Venus (Fox and Victor, 1981). However, the total O^{++} production rate is significantly higher than the total destruction rate, with a difference by more than a factor of 20 at 300 km. The possible reasons for such a difference are discussed in Section 4 below.

4. Discrepancy Between O^{++} Production and Destruction Above 200 km

The comparison between the O^{++} production and destruction rates is subject to a number of uncertainties, which we address in turn below.

First, charge exchange reaction with O_2 likely serves as an important destruction channel of O^{++} in the ionospheres of both the Earth and Venus (Victor and Constantinides, 1979; Fox and Victor, 1981), but such a process is ignored in our calculations mainly due to the lack of available O_2 densities in the publicly available NGIMS level 2 data. Based on the early NGIMS measurements, Mahaffy et al. (2015b) reported the observation of O_2 in the dayside Martian upper atmosphere, with a vertical density profile comparable to those of N_2 and CO (see their Figure 5). If we take Mahaffy et al.'s O_2 profile as representative of the dayside median situation, we may conclude that the contribution to the O^{++} destruction from charge exchange with O_2 is comparable to the contribution from charge exchange with either N_2 or CO. Accordingly, including O_2 may slightly increase the total O^{++} destruction rate but should not have any appreciable impact on the overall O^{++} balance in the dayside Martian ionosphere as outlined in Section 3.

Second, the NGIMS-derived O densities might be seriously overestimated due to the strong wall contamination of this species (Stone et al., 2018), even though only the inbound O measurements are considered here. For instance, Mahaffy et al. (2015b) reported that O density of approximately 10^7 cm^{-3} near 300 km, which is more than a factor of 10 higher than the value derived from observations made by the Mars Express Spectroscopy for the Investigation of the Characteristics of the Atmosphere of Mars (e.g., Chaufray et al., 2009). However, this uncertainty should not influence the O^{++} balance at high altitudes because a change in the ambient O density modifies proportionally both the O^{++} production and destruction rates, leaving the observed discrepancy from local PCE above 200 km essentially unaffected.

Third, the O^{++} destruction rate via charge exchange with O is calculated in this study with the rate coefficient of Fox and Victor (1981), which was estimated from theoretical considerations of O^{++} balance in the Venusian ionosphere rather than obtained from laboratory experiments. If instead we require strict local PCE above 200 km in the dayside Martian ionosphere, the actual rate coefficient should be substantially higher than the Fox and Victor's value, but this would also proportionally raise the total O^{++} destruction rate near and below 200 km to be well above the total O^{++} production rate. Therefore it is clear that the condition of local PCE cannot be simultaneously satisfied in both the upper and lower portions of the dayside Martian ionosphere displayed in Figure 2.

The above discussion leads us to suggest that the break of local PCE above 200 km is very likely a realistic feature, which could be interpreted as a signature of strong O^{++} transport in the dayside Martian ionosphere. Similar to Cui J et al. (2010), we estimate the characteristic column integrated difference between the O^{++} production and destruction rates above 200 km to be 8×10^4 cm^{-2} s^{-1} referred to an altitude of 300 km on the dayside of Mars, or equivalently a total O^{++} outflow rate of 7×10^{22} s^{-1} when summed over the entire dayside hemisphere. Such an outflow should be the combined result of cold plasma escape from Mars (e.g., Chen RH et al., 1978; Kar et al., 1996; Fox, 1997, 2009; Wu XS et al., 2019)

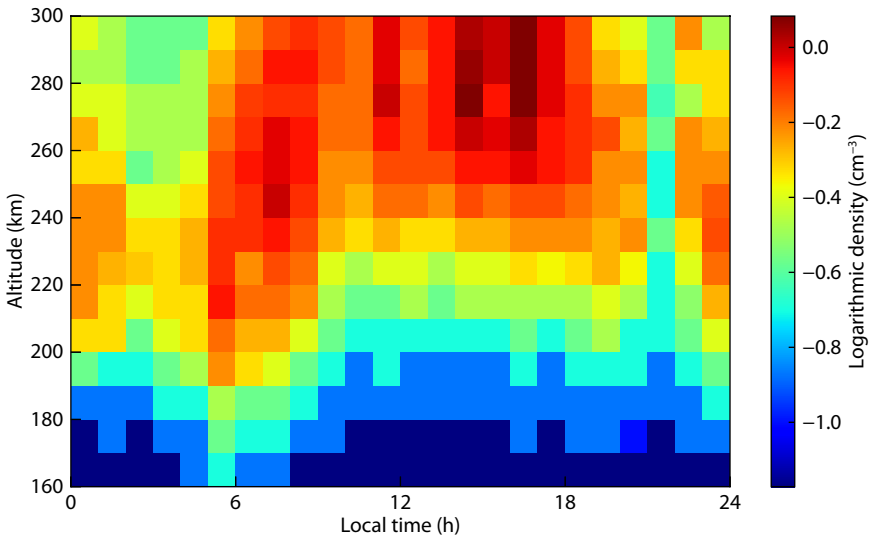

Figure 3. The diurnal variation of O^{++} density in the Martian ionosphere based on available MAVEN NGMIS measurements.

and horizontal plasma transport that sustains an ionosphere beyond the terminator (e.g., Withers et al., 2012; Cui J et al., 2015; Girazian et al., 2017a; Cao YT et al., 2019). The diurnal variation of O^{++} density in the Martian ionosphere at 160–300 km is presented in Figure 3 for reference, constructed from all available NGIMS data.

Similar to the dayside calculations, we use the NGIMS measurements of O^{++}, CO_2, O, N_2, and CO at SZA > 110° to obtain a total O^{++} destruction rate via charge exchange, given by the black crosses in Figure 2. When integrated above 200 km and summed over the nightside hemisphere, we estimate the total O^{++} destruction rate in the nightside Martian ionosphere to be 9×10^{21} s^{-1}. This means that a substantial fraction of more than 85% of the dayside O^{++} outflow rate, which is about 6×10^{22} s^{-1}, reflects essentially an O^{++} escape rate. In reality, a portion of O^{++} destruction in the nightside Martian ionosphere should be balanced by impact ionization of atmospheric O by precipitating energetic electrons (e.g., Fowler et al., 2015; Girazian et al., 2017b; Cui J et al., 2019). If this is taken into account, we may interpret the 6×10^{22} s^{-1} quoted above as an upper limit to the total O^{++} escape rate on Mars.

5. Concluding Remarks

O^{++} has been observed in the dayside ionospheres of both the Earth (Breig et al., 1977) and Venus (Taylor et al., 1980). Previous studies have suggested the O^{++} photochemistry to be manifest as production via both photoionization of O^+ and double photoionization of O, and destruction via charge exchange with ambient neutrals (e.g., Victor and Constantinides, 1979; Fox and Victor, 1981). The recent measurements made by the NGIMS instrument on board MAVEN provide the first firm detection of O^{++} in the Martian ionosphere (Benna et al., 2015), allowing the O^{++} photochemistry proposed in previous studies to be validated.

Based on the NGIMS measurements of relevant neutral and ion species accumulated over a large number of MAVEN orbits, we calculate in this study the O^{++} production and destruction rates in the dayside Martian ionosphere. Our calculations reveal the dominant O^{++} production channels to be double photoionization of O at low altitudes and photoionization of O^+ at high altitudes, respectively, reflecting a varying degree of O ionization (Bougher et al., 2015). In the dayside median sense, total O^{++} production is exactly balanced by total O^{++} destruction via charge exchange with several ambient neutral species, for which charge exchange with CO_2 dominates at low altitudes and charge exchange with O dominates at high altitudes in response to the varying O mixing ratio in the Martian upper atmosphere (Mahaffy et al., 2015a). By excluding several possibilities such as the unknown contribution of charge exchange with O_2 (Victor and Constantinides, 1979), the strong wall contamination of O (Stone et al., 2018), as well as the uncertainty in some of the rate coefficients (Fox and Victor, 1981), we argue that the apparent break of local PCE above 200 km is a real feature, which we interpret as a signature of strong O^{++} escape on Mars (e.g., Fox, 2009; Wu XS et al., 2019). The total O^{++} escape rate is estimated to be 6×10^{22} s^{-1} based on an evaluation of O^{++} balance throughout the entire ionosphere of Mars.

Our evaluation of O^{++} balance in the dayside Martian upper atmosphere generally confirms the photochemical scheme of this doubly charged species previously proposed based on ionospheric observations made on both the Earth (Breig et al., 1977) and Venus (Fox and Victor, 1981). However, the distinctive discrepancy between O^{++} production and destruction suggests strong O^{++} outflow on Mars, a feature that has not been reported on the other two terrestrial planets.

Acknowledgments

The authors acknowledge support from the National Natural Science Foundation of China (NSFC) through grants 41525015, 41774186, 41704160, and 41804150. The data used in this study are publicly available at the MAVEN Science Data Center (https://lasp.colorado.edu/maven/sdc/public/). We appreciate the two anonymous referees for their constructive comments which have greatly improved the quality of the manuscript.

References

Benna, M., Mahaffy, P. R., Grebowsky, J. M., Fox, J. L., Yelle, R. V., and Jakosky, B. M. (2015). First measurements of composition and dynamics of the Martian ionosphere by MAVEN's Neutral Gas and Ion Mass Spectrometer. *Geophys. Res. Lett.*, *42*(21), 8958–8965. https://doi.org/10.1002/2015GL066146

Bougher, S., Jakosky, B., Halekas, J., Grebowsky, J., Luhmann, J., Mahaffy, P., Connerney, J., Eparvier, F., Ergun, R.,... Yelle, R. V. (2015). Early MAVEN deep dip campaign reveals thermosphere and ionosphere variability. *Science*, *350*(6261), aad0459. https://doi.org/10.1126/science.aad0459

Breig, E. L., Torr, M. R., Torr, D. G., Hanson, W. B., Hoffman, J. H., Walker, J. G. G., and Nier, A. O. (1977). Doubly charged atomic oxygen ions in the thermosphere, 1. Photochemistry. *J. Geophys. Res. Space Phys.*, *82*(7), 1008–1012. https://doi.org/10.1029/JA082i007p01008

Breig, E. L., Torr, M. R., and Kayser, D. C. (1982). Observations and photochemistry of O^{++} in the daytime thermosphere. *J. Geophys. Res. Space Phys.*, *87*(A9), 7653–7665. https://doi.org/10.1029/JA087iA09p07653

Cao, Y. T., Cui, J., Wu, X. S., Guo, J. P., and Wei, Y. (2019). Structural variability of the nightside Martian ionosphere near the terminator: implications on plasma sources. *J. Geophys. Res. Planets*, *124*(E6), 1495–1511. https://doi.org/10.1029/2019JE005970

Chaufray, J. Y., Leblanc, F., Quémerais, E., and Bertaux, J. L. (2009). Martian oxygen density at the exobase deduced from OI 130.4-nm observations by Spectroscopy for the Investigation of the Characteristics of the Atmosphere of Mars on Mars Express. *J. Geophys. Res. Planets*, *114*(E2). https://doi.org/10.1029/2008JE003130

Chen, R. H., Cravens, T. E., and Nagy, A. F. (1978). The Martian ionosphere in light of the Viking observations. *J. Geophys. Res. Space Phys.*, *83*(A8), 3871–3876. https://doi.org/10.1029/JA083iA08p03871

Connerney, J. E. P., Acuña, M. H., Wasilewski, P. J., Ness, N. F., Rème, H., Mazelle, C., Vignes, D., Lin, R. P., Mitchell, D. L., and Cloutier, P. A. (1999). Magnetic lineations in the ancient crust of Mars. *Science*, *284*(5415), 794–798. https://doi.org/10.1126/science.284.5415.794

Cui, J., Galand, M., Yelle, R. V., Wahlund, J.-E., Ågren, K., Waite, Jr. J. H., and Dougherty, M. K. (2010). Ion transport in Titan's upper atmosphere. *J. Geophys. Res. Space Phys.*, *115*(A6), A06314. https://doi.org/10.1029/2009JA014563

Cui, J., Galand, M., Coates, A. J., Zhang, T. L., and Müller-Wodarg, I. C. F. (2011). Suprathermal electron spectra in the Venus ionosphere. *J. Geophys. Res. Space Phys.*, *116*(A4), A04321. https://doi.org/10.1029/2010JA016153

Cui, J., Galand, M., Zhang, S. J., Vigren, E., and Zou, H. (2015). The electron thermal structure in the dayside Martian ionosphere implied by the MGS radio occultation data. *J. Geophys. Res. Planets*, *120*(E2), 278–286. https://doi.org/10.1002/2014JE004726

Cui, J., Cao, Y. T., Wu, X. S., Xu, S. S., Yelle, R. V., Stone, S., Vigren, E., Edberg, N. J. T., Shen, C. L., … and Wei, Y. (2019). Evaluating local ionization balance in the nightside Martian upper atmosphere during MAVEN Deep Dip

campaigns. *Astrophys. J. Lett.*, *876*(1), L12. https://doi.org/10.3847/2041-8213/ab1b34

Eparvier, F. G., Chamberlin, P. C., Woods, T. N., and Thiemann, E. M. B. (2015). The solar extreme ultraviolet monitor for MAVEN. *Space Sci. Rev.*, *195*(1-4), 293–301. https://doi.org/10.1007/s11214-015-0195-2

Fowler, C. M., Andersson, L., Ergun, R. E., Morooka, M., Delory, G., Andrews, D. J., Lillis, R. J., McEnulty, T., Weber, T. D.,... Jakosky, B. M. (2015). The first in situ electron temperature and density measurements of the Martian nightside ionosphere. *Geophys. Res. Lett.*, *42*(1), 8854–8861. https://doi.org/10.1002/2015GL065267

Fox, J. L., and Victor, G. A. (1981). O^{++} in the Venusian ionosphere. *J. Geophys. Res. Space Phys.*, *86*(A4), 2438–2442. https://doi.org/10.1029/JA086iA04p02438

Fox, J. L. (1997). Upper limits to the outflow of ions at Mars: Implications for atmospheric evolution. *Geophys. Res. Lett.*, *24*(22), 2901–2904. https://doi.org/10.1029/97GL52842

Fox, J. L. (2009). Morphology of the dayside ionosphere of Mars: Implications for ion outflows. *J. Geophys. Res. Planets*, *114*(E12), E12005. https://doi.org/10.1029/2009JE003432

Geiss, J., Balsiger, H., Eberhardt, P., Walker, H. P., Weber, L., Young, D. T., and Rosenbauer, H. (1978). Dynamics of magnetospheric ion composition as observed by the GEOS mass spectrometer. *Space Sci. Rev.*, *22*(5), 537–566. https://doi.org/10.1007/BF00223940

Geiss, J., and Young, D. T. (1981). Production and transport of O^{++} in the ionosphere and plasmasphere. *J. Geophys. Res. Space Phys.*, *86*(A6), 4739–4750. https://doi.org/10.1029/JA086iA06p04739

Ghosh, S., Mahajan, K. K., Grebowsky, J. M., and Nath, N. (1995). Morphology of O^{++} ions and their maintenance in the nightside Venus ionosphere. *J. Geophys. Res. Space Phys.*, *100*(A12), 23983–23991. https://doi.org/10.1029/95JA01581

Girazian, Z., Mahaffy, P. R., Lillis, R. J., Benna, M., Elrod, M., and Jakosky, B. M. (2017a). Nightside ionosphere of Mars: Composition, vertical structure, and variability. *J. Geophys. Res. Space Phys.*, *122*(A4), 4712–4725. https://doi.org/10.1002/2016JA023508

Girazian, Z., Mahaffy, P., Lillis, R. J., Benna, M., Elrod, M., Fowler, C. M., and Mitchell, D. L. (2017b). Ion densities in the nightside ionosphere of Mars: Effects of electron impact ionization. *Geophys. Res. Lett.*, *44*(22), 11248–11256. https://doi.org/10.1002/2017GL075431

Hedin, A. E. (1983). A revised thermospheric model based on mass spectrometer and incoherent scatter data: MSIS-83. *J. Geophys. Res. Space Phys.*, *88*(A12), 10170–10188. https://doi.org/10.1029/JA088iA12p10170

Henry, R. J. W. (1968). Photoionization cross sections for N and O+. *J. Chem. Phys.*, *48*(8), 3635–3638. https://doi.org/10.1063/1.1669662

Howorka, F., Viggiano, A. A., Albritton, D. L., Ferguson, E. E., and Fehsenfeld, F. C. (1979). Laboratory studies of O^{++} reactions of ionospheric importance. *J. Geophys. Res. Space Phys.*, *84*(A10), 5941–5942. https://doi.org/10.1029/JA084iA10p05941

Jakosky, B. M., Grebowsky, J. M., Luhmann, J. G., and Brain, D. A. (2015). Initial results from the MAVEN mission to Mars. *Geophys. Res. Lett.*, *42*(21), 8791–8802. https://doi.org/10.1002/2015GL065271

Johnsen, R., and Biondi, M. A. (1978). Measurements of the reaction rates of O^{++} ions with N_2 and O_2 at thermal energy and their ionospheric implications. *Geophys. Res. Lett.*, *5*(10), 847–848. https://doi.org/10.1029/GL005i010p00847

Kar, J., Mahajan, K. K., and Kohli, R. (1996). On the outflow of O_2^+ ions at Mars. *J. Geophys. Res. Planets*, *101*(E5), 12747–12752. https://doi.org/10.1029/95JE03526

Laher, R. R., and Gilmore, F. R. (1990). Updated excitation and ionization cross sections for electron impact on atomic oxygen. *J. Phys. Chem. Ref. Data*, *19*(1), 277–305. https://doi.org/10.1063/1.555872

Mahaffy, P. R., Benna, M., Elrod, M., Yelle, R. V., Bougher, S. W., Stone, S. W., and Jakosky, B. M. (2015a). Structure and composition of the neutral upper atmosphere of Mars from the MAVEN NGIMS investigation. *Geophys. Res. Lett.*, *42*(21), 8951–8957. https://doi.org/10.1002/2015GL065329

Mahaffy, P. R., Benna, M., King, T., Harpold, D. N., Arvey, R., Barciniak, M., Bendt, M., Carrigan, D., Errigo, T., … Nolan, J. T. (2015b). The neutral gas and ion mass spectrometer on the mars atmosphere and volatile evolution mission. *Space Sci. Rev.*, *195*(1-4), 59–73. https://doi.org/10.1007/s11214-014-0091-1

Stone, S. W., Yelle, R. V., Benna, M., Elrod, M. K., and Mahaffy, P. R. (2018). Thermal structure of the Martian upper atmosphere from MAVEN NGIMS. *J. Geophys. Res. Planets*, *123*(11), 2842–2867. https://doi.org/10.1029/2018JE005559

Taylor, Jr. H. A., Brinton, H. C., Bauer, S. J., Hartle, R. E., Cloutier, P. A., and Daniell, Jr. R. E. (1980). Global observations of the composition and dynamics of the ionosphere of Venus: Implications for the solar wind interaction. *J. Geophys. Res. Space Phys.*, *85*(A13), 7765–7777. https://doi.org/10.1029/JA085iA13p07765

Thiemann, E. M. B., Chamberlin, P. C., Eparvier, F. G., Templeman, B., Woods, T. N., Bougher, S. W., and Jakosky, B. M. (2017). The MAVEN EUVM model of solar spectral irradiance variability at Mars: Algorithms and results. *J. Geophys. Res. Space Phys.*, *122*(3), 2748–2767. https://doi.org/10.1002/2016JA023512

Thissen, R., Witasse, O., Dutuit, O., Wedlund, C. S., Gronoff, G., and Lilensten, J. (2011). Doubly-charged ions in the planetary ionospheres: a review. *Phys. Chem. Chem. Phys.*, *13*(41), 18264–18287. https://doi.org/10.1039/C1CP21957J

Victor, G. A., and Constantinides, E. R. (1979). Double photoionization and doubly charged ions in the thermosphere. *Geophys. Res. Lett.*, *6*(6), 519–522. https://doi.org/10.1029/GL006i006p00519

Withers, P., Fallows, K., Girazian, Z., Matta, M., Häusler, B., Hinson, D., Tyler, L., Morgan, D., Pätzold, M.,... Witasse, O. (2012). A clear view of the multifaceted dayside ionosphere of Mars. *Geophys. Res. Lett.*, *39*(18), L18202. https://doi.org/10.1029/2012GL053193

Wu, X. S., Cui, J., Xu, S. S., Lillis, R. J., Yelle, R. V., Edberg, N. J. T., Vigren, E., Rong, Z. J., Fan, K., … Mitchell, D. L. (2019). The morphology of the topside Martian ionosphere: implications on bulk ion flow. *J. Geophys. Res. Planets*, *124*(3), 734–751. https://doi.org/10.1029/2018JE005895